The *Drosophila* clock neuron network features diverse coupling modes and requires network-wide coherence.

Supplementary Material

Zepeng Yao, Amelia J Bennett, Jenna L Clem, Orie T Shafer[1,2]

Department of Molecular Cellular and Developmental Biology, University of Michigan, Ann Arbor, MI 48109

[1] Corresponding Author (oshafer@umich.edu); [2]Lead Contact

Supplemental Experimental Procedures

Fly strains

All of the fly strains used in this study have been described previously, they are: *UAS-DBT^{S}(10F5A)* and *UAS-DBT^{L}(22F1C)(Muskus et al., 2007)*, *UAS-SGG^{Y214F}(hypomorphic SGG mutant)* (Bloomington Stock # 6817) (Bourouis, 2002; Yao and Shafer, 2014), *nSyb-GAL4* (Pauli et al., 2008), *Pdf-GAL4* (Park et al., 2000; Renn et al., 1999), *Clk4.1M-GAL4* (Zhang et al., 2010a; Zhang et al., 2010b), *Mai179-GAL4* (Grima et al., 2004; Siegmund and Korge, 2001), *Pdf-GAL80* (Stoleru et al., 2004), and *DvPdf-GAL4* (Bahn et al., 2009). Given the fact that the specific *GAL4* lines used in this study were expressed in subsets of neurons, we reasoned that the use of the pan-neuronal driver *nSyb-GAL4* to speed-up and slow-down all neuronal clocks would be the most reasonable means of measuring features of the activity rhythms when the entire neural network was uniformly manipulated without affecting non neuronal cell types. We therefore compared the effects of manipulating subsets of neurons to the effects of *nSyb-GAL4* driven manipulations across the network.

Manipulations driven by the widespread and commonly used clock drivers *timeless-GAL4* and *Clock(856)-GAL4* produced highly similar effects (data not shown).

Locomotor activity rhythm recording and analysis

Locomotor activity rhythms of adult male flies were recorded using the TriKinetics DAM2 monitors (Waltham, MA) as described previously (Pfeiffenberger et al., 2010; Yao and Shafer, 2014). Flies aged a week or less were placed individually in recording glass tubes containing 2% agar-4% sucrose food, and these were loaded onto the DAM2 monitors for locomotor activity recording. Flies were entrained to 12:12 LD cycles for at least 5 days, and subsequently released into constant darkness (DD) for at least 7 days, at a constant temperature of 25°C. Activity counts were collected in either 5-minute or 1-minute bins that were subsequently summed into 30-minute bins for time-series analysis. Averaged population activity profiles (also known as "eduction plots") of specific genotypes in LD were generated using the Counting Macro, an Excel-based program, which has been described previously (Pfeiffenberger et al., 2010). First, activity levels were normalized among individual flies, such that for each individual fly the average activity value of all bins for the last four days in LD equals 1. Second, the population average of normalized activity is determined for any given 30-min bin for the last four days in LD. Finally, the population activity for these four days is averaged into a single 24-hour day, and the results are displayed in the figures. Averaged population activity profiles in DD1 were generated in the same way except that only data of the first day in DD were used.

The analysis of free-running activity rhythms was done using the ClockLab software from Actimetrics (Wilmette, IL) as previously described (Yao and Shafer, 2014). In brief, rhythmicity and free-running period of individual flies were determined using the χ-square periodogram function implemented in ClockLab, with a confidence level of 0.01 (Sokolove and Bushell, 1978). For all the

genotypes, the range of free-running periods analyzed was from 14 hours to 34 hours, with 0.5-hour intervals. For individuals with more than one significant period, only the period with the highest amplitude over significance was used for the scatter plots of free-running periods in the figures and the determination of average periods in Table S2. For each significant period, the χ-square analysis in Clock Lab returns a "Power" value and a "Significance" value. "Rhythmic Power" was calculated as "Rhythmic Power = Power – Significance" for rhythmic flies, and considered "0" for arrhythmic flies, as previously described (Pfeiffenberger et al., 2010; Yao and Shafer, 2014). The statistical methods used in Figures S3 and S4 are described in the figure legends.

Immunocytochemistry

Immunostaining of whole-mount *Drosophila* brains was done as previously described (Yao and Shafer, 2014). Dissected brains were fixed in 4% paraformaldehyde for 1 hour at room temperature, blocked with 3% normal goat serum for 1 hour at room temperature, and stained with rat anti-PER antibodies (1:500) (provided by Dr. Michael Rosbash, (Liu et al., 1988)) at 4 °C for two nights and then rinsed in PBS-TX. LN_vs (morning oscillator) were identified by co-staining the brains with mouse anti-PDF antibodies (1:200) (Developmental Studies Hybridoma Bank, contributed by Dr. Justin Blau). CRY^+ $DN1_p$s were identified by co-staining the brains with rabbit anti-CRY antibodies (1:500) (provided by Dr. Charlotte Helfrich-Förster, (Yoshii et al., 2008)). Alexa Fluor conjugated secondary antibodies were used at 1:1000 (Invitrogen, Grand Island, NY) at 4 °C overnight and then rinsed in PBS-TX. Brains were mounted for imaging in Vectashield HardSet Mounting Medium (Vector Laboratories, Burlingame, CA). All samples were imaged on an Olympus Fluoview 1000 confocal microscope with a 60×/1.10 NA objective (Olympus, Center Valley, PA). Imaging settings were tailored for each class of clock neurons, but were kept constant for all time points and genotypes within a neuronal class. PER immunostaining intensity of individual clock

neurons was quantified using the ImageJ software (National Institutes of Health, USA) as previously described (Shafer et al., 2002). Both hemispheres of about ten brains were used for quantification at each time point.

Supplemental References

Bahn, J.H., Lee, G., and Park, J.H. (2009). Comparative analysis of Pdf-mediated circadian behaviors between Drosophila melanogaster and D. virilis. Genetics *181*, 965-975.
Bourouis, M. (2002). Targeted increase in shaggy activity levels blocks wingless signaling. genesis *34*, 99-102.
Grima, B., Chelot, E., Xia, R., and Rouyer, F. (2004). Morning and evening peaks of activity rely on different clock neurons of the Drosophila brain. Nature *431*, 869-873.
Liu, X., Lorenz, L., Yu, Q.N., Hall, J.C., and Rosbash, M. (1988). Spatial and temporal expression of the period gene in Drosophila melanogaster. Genes & Development *2*, 228-238.
Muskus, M.J., Preuss, F., Fan, J.-Y., Bjes, E.S., and Price, J.L. (2007). Drosophila DBT Lacking Protein Kinase Activity Produces Long-Period and Arrhythmic Circadian Behavioral and Molecular Rhythms. Molecular and Cellular Biology *27*, 8049-8064.
Park, J.H., Helfrich-Forster, C., Lee, G., Liu, L., Rosbash, M., and Hall, J.C. (2000). Differential regulation of circadian pacemaker output by separate clock genes in Drosophila. Proc Natl Acad Sci U S A *97*, 3608-3613.
Pauli, A., Althoff, F., Oliveira, R.A., Heidmann, S., Schuldiner, O., Lehner, C.F., Dickson, B.J., and Nasmyth, K. (2008). Cell-type-specific TEV protease cleavage reveals cohesin functions in Drosophila neurons. Dev Cell *14*, 239-251.
Pfeiffenberger, C., Lear, B.C., Keegan, K.P., and Allada, R. (2010). Processing Circadian Data Collected from the Drosophila Activity Monitoring (DAM) System. Cold Spring Harbor Protocols *2010*, pdb.prot5519.
Renn, S.C.P., Park, J.H., Rosbash, M., Hall, J.C., and Taghert, P.H. (1999). A pdf Neuropeptide Gene Mutation and Ablation of PDF Neurons Each Cause Severe Abnormalities of Behavioral Circadian Rhythms in Drosophila. Cell *99*, 791-802.
Shafer, O.T., Rosbash, M., and Truman, J.W. (2002). Sequential Nuclear Accumulation of the Clock Proteins Period and Timeless in the Pacemaker Neurons of Drosophila melanogaster. J Neurosci *22*, 5946-5954.
Siegmund, T., and Korge, G. (2001). Innervation of the ring gland of Drosophila melanogaster. The Journal of Comparative Neurology *431*, 481-491.
Sokolove, P.G., and Bushell, W.N. (1978). The chi square periodogram: Its utility for analysis of circadian rhythms. Journal of Theoretical Biology *72*, 131-160.
Stoleru, D., Peng, Y., Agosto, J., and Rosbash, M. (2004). Coupled oscillators control morning and evening locomotor behaviour of Drosophila. Nature *431*, 862-868.
Yao, Z., and Shafer, O.T. (2014). The Drosophila Circadian Clock Is a Variably Coupled Network of Multiple Peptidergic Units. Science *343*, 1516-1520.

Yoshii, T., Todo, T., Wülbeck, C., Stanewsky, R., and Helfrich-Förster, C. (2008). Cryptochrome is present in the compound eyes and a subset of Drosophila's clock neurons. The Journal of Comparative Neurology *508*, 952-966.
Zhang, L., Chung, B.Y., Lear, B.C., Kilman, V.L., Liu, Y., Mahesh, G., Meissner, R.-A., Hardin, P.E., and Allada, R. (2010a). DN1p Circadian Neurons Coordinate Acute Light and PDF Inputs to Produce Robust Daily Behavior in Drosophila. Current Biology *20*, 591-599.
Zhang, Y., Liu, Y., Bilodeau-Wentworth, D., Hardin, P.E., and Emery, P. (2010b). Light and Temperature Control the Contribution of Specific DN1 Neurons to Drosophila Circadian Behavior. Current biology : CB *20*, 600-605.

Supplemental Figures and Legends

Figure S1

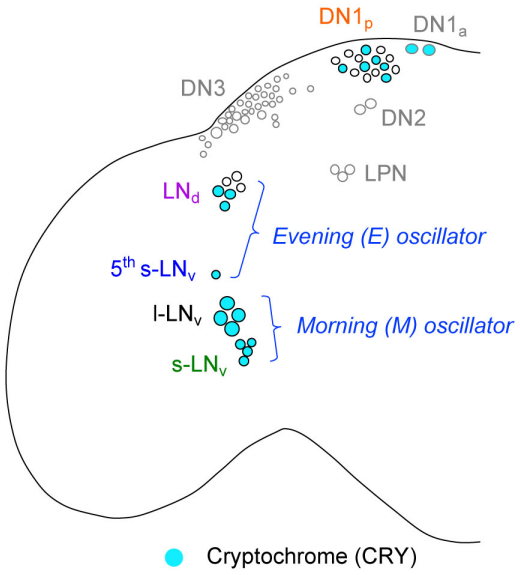

Figure S1. A diagram of the *Drosophila* clock neuron network. Related to Figures 1-4.

The cell bodies of the different groups of clock neurons are illustrated for the left hemisphere of the adult *Drosophila* brain. The neuronal groups that this study mainly focuses on are labelled in colors to match those shown in Figure 2D-E and Figure 3A. Neurons that express the circadian photoreceptor cryptochrome are shown in cyan. In the classical dual-oscillator model, the s-LN$_v$s and l-LN$_v$s as a group are considered the morning oscillator, while the LN$_d$s and 5th s-LN$_v$ as a group are considered the evening oscillator (see text for more details).

Figure S2

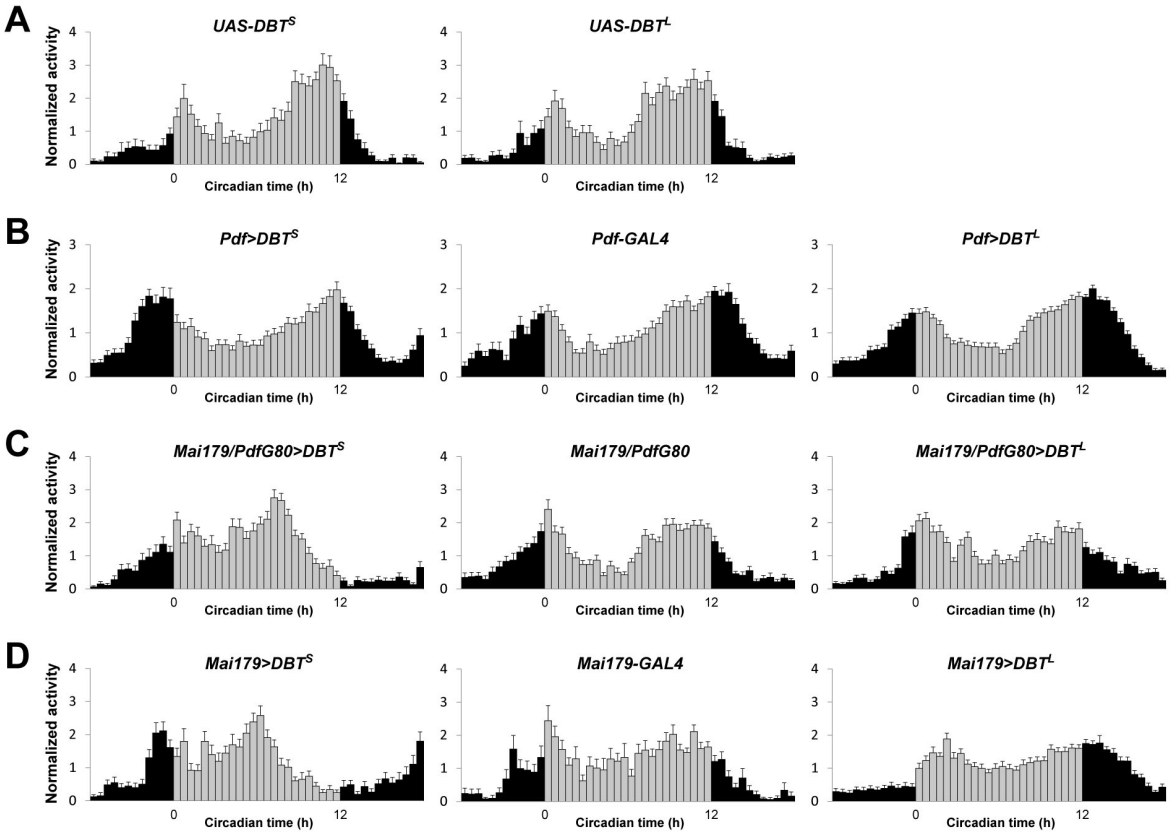

Figure S2. Group averaged activity profiles of the various genotypes shown in Figure 2A-C. Related to Figure 2.

(A-D) Population averaged activity profiles of the indicated genotypes in DD1. The gray bars indicate the subjective light period and the black bars indicate the subjective dark period. The behavior of parental UAS controls is shown in (A). Genetic manipulations were targeted to the morning oscillator in (B), the evening oscillator in (C), and both morning and evening oscillators in (D). See Table S1 for expression pattern of each genetic driver.

Figure S3

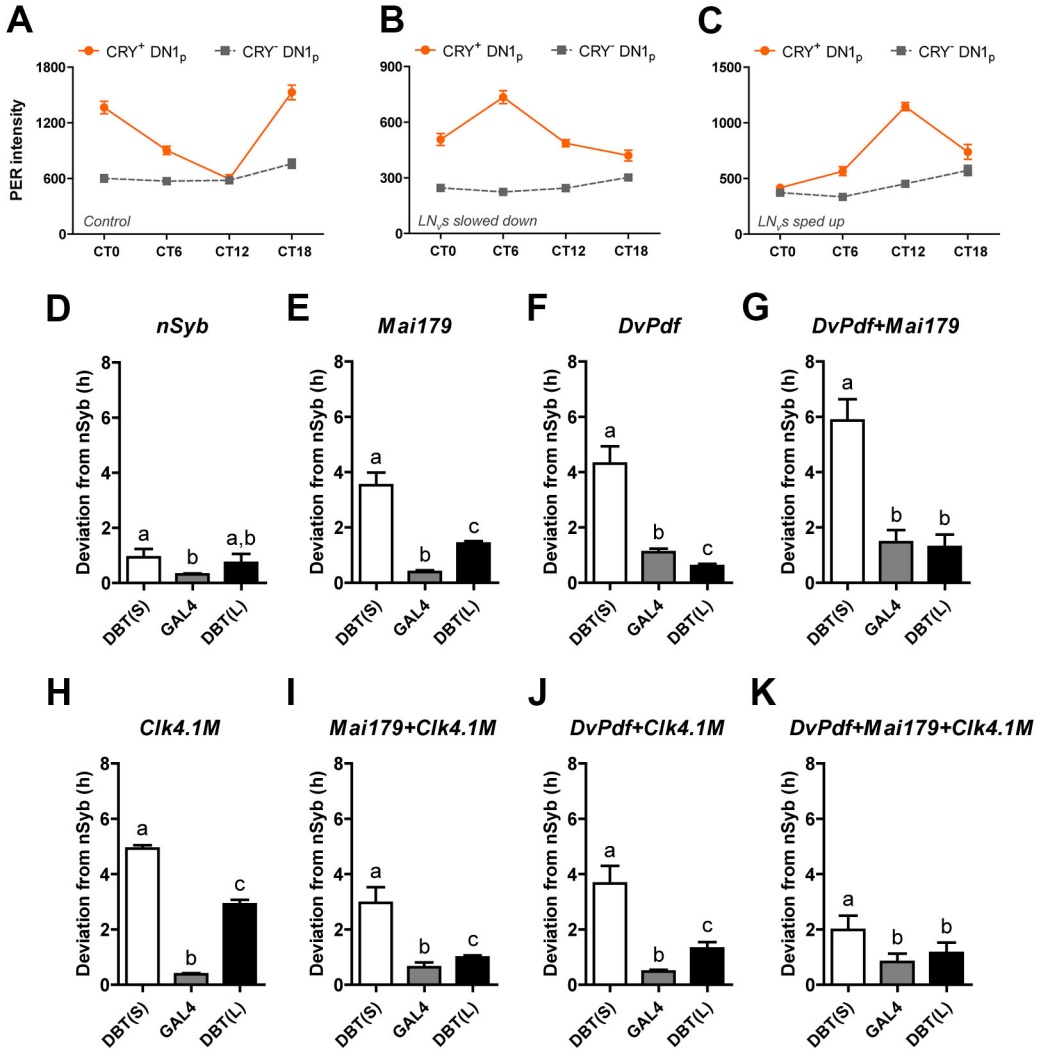

Figure S3. PER expression in the CRY+ ad CRY- DN1$_p$s and Deviation of free-running periods for each *GAL4* manipulation from expected free-running periods. Related to Figures 2-4.

(A-C) PER immunostaining intensity of the CRY$^+$ DN1$_p$s and CRY$^-$ DN1$_p$s of *Pdf-GAL4* flies (A), *Pdf>DBT^L* flies (B), and *Pdf>DBT^S* flies (C) under the same image acquisition settings. (D-K) The absolute deviation of free-running periods from the expected periods for *GAL4* control flies and flies overexpressing *DBT^S* and *DBT^L* under the indicated drivers. The means of the free-running periods of the *nSyb-GAL4* manipulations are taken as the expected free-running periods, i.e. the expected

period for *DBT*^{S} overexpression is 18.5h, for *DBT*^{L} overexpression 26.9h, and for *GAL4* control 23.8h. For each *GAL4* manipulation, the absolute deviation (without signs) of free-running periods from the respective expected period was calculated and plotted as mean ± SEM in the graphs. A small deviation value indicates that the free-running periods are close to the expected period for that specific manipulation. For each panel, groups that do not share a letter ("a", "b", or "c") are significantly different from each other ($P < 0.05$, by Kruskal-Wallis one-way ANOVA and Dunn's multiple comparisons test).

Figure S4

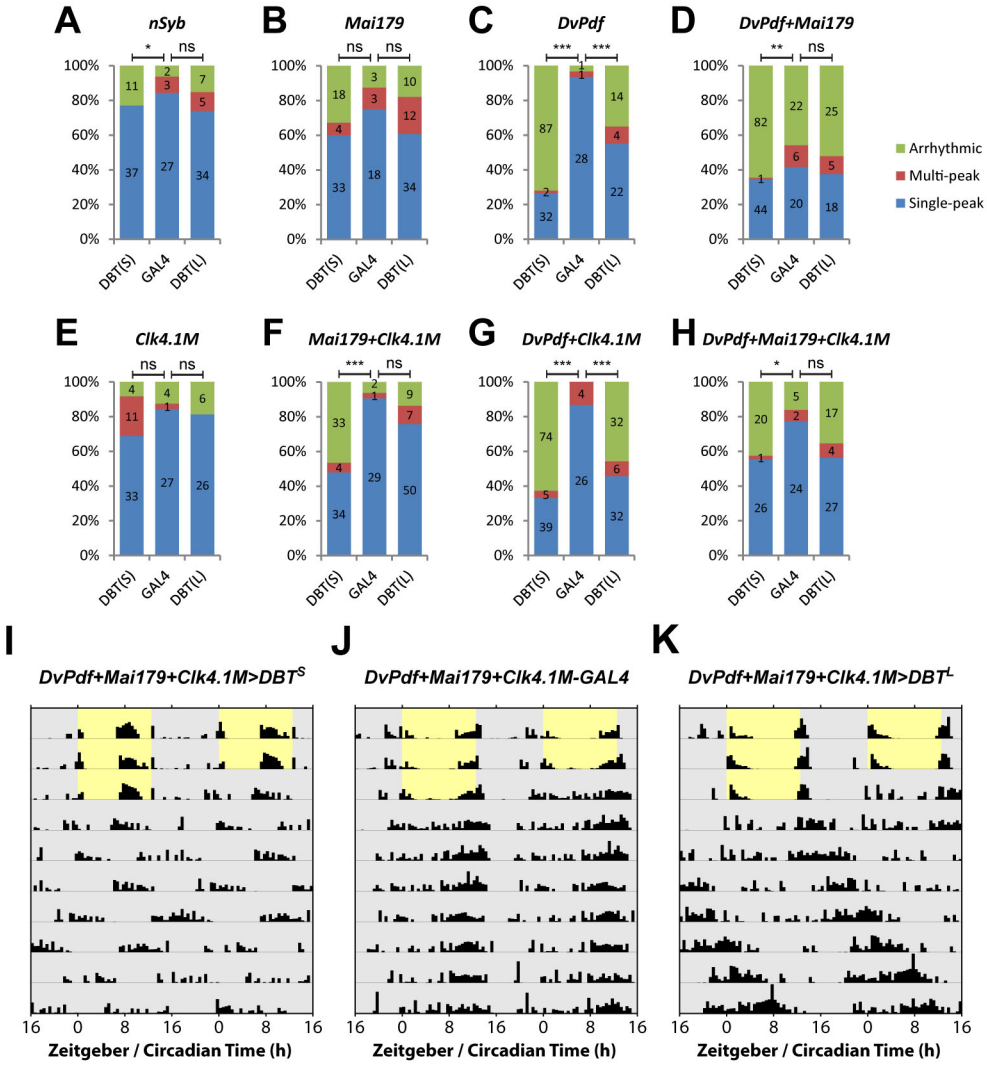

Figure S4. Rhythmicity and internal desynchronization of free-running rhythms for each *GAL4* manipulation. Related to Figures 2-4.

(A-H) The percentages of arrhythmic flies (green), rhythmic flies displaying a single significant period (blue), and rhythmic flies displaying multiple significant periods (red) for *GAL4* control flies and flies overexpressing DBT^S and DBT^L under the indicated drivers. The numbers of flies in each category are displayed on each bar of the histogram. * $P < 0.05$; ** $P < 0.01$; *** $P < 0.001$; ns, not

significant, by the Freeman-Halton extension of the Fisher's exact test. (I-K) Manipulation of the CRY$^+$ DN1$_p$s and all of the lateral clock neurons together are capable of more coherently resetting free-running activity rhythms than the manipulation of lateral neurons alone. Representative individual actograms of the *GAL4* control (J) and flies overexpressing *DBT^S* (I) and *DBT^L* (K) in the CRY$^+$ DN1$_p$s and all of the lateral clock neurons, through a combined use of *DvPdf-GAL4*, *Mai179-GAL4*, and *Clk4.1M-GAL4* drivers (Table S1). The actograms are double-plotted for two consecutive days. Yellow indicates light and gray indicates darkness.

Table S1. Expression patterns of *GAL4* drivers. Related to Figures 1-4.

GAL4 driver	Expression pattern
nSyb-GAL4	All neurons (Pauli et al., 2008)
Pdf-GAL4	l-LN$_v$s, s-LN$_v$s (Park et al., 2000; Renn et al., 1999)
Clk4.1M-GAL4	High expression in ~4-5 DN1$_p$s, weaker expression in another ~4-5 DN1$_p$s; the majority express CRY (Zhang et al., 2010a; Zhang et al., 2010b).
Mai179-GAL4	s-LN$_v$s, 3 CRY$^+$ LN$_d$s, 5th s-LN$_v$, weak and variable expression in l-LN$_v$s, DN1s, and many non-clock neurons (Grima et al., 2004; Picot et al., 2007; Shafer and Taghert, 2009; Yoshii et al., 2008).
Mai179-GAL4/Pdf-GAL80	3 CRY$^+$ LN$_d$s, 5th s-LN$_v$, and many non-clock neurons
DvPdf-GAL4	l-LN$_v$s, s-LN$_v$s, 4 LN$_d$s (1 CRY$^+$, 3CRY$^-$), 5th s-LN$_v$ (Bahn et al., 2009; Guo et al., 2014)

Table S2. Summary of free-running locomotor activity rhythms. Related to Figures 1-4.

Genotype	Number of flies	% Rhythmic	% Multi-periodicity*	Period ± SEM (h)	Rhythmic Power ± SEM
;;UAS-DBT(S)/+	37	94.6	0	23.5 ± 0.1	54.4 ± 7.2
;;UAS-DBT(L)/+	44	97.7	7.0	23.6 ± 0.2	72.9 ± 6.2
;;nSyb-GAL4/+	32	93.8	10.0	23.8 ± 0.1	41.7 ± 8.1
;;nSyb-GAL4/UAS-DBT(S)	48	77.1	0	18.5 ± 0.3	21.7 ± 3.7
;;nSyb-GAL4/UAS-DBT(L)	46	84.8	12.8	26.9 ± 0.3	33.6 ± 5.3
;;Clk4.1M-GAL4/+	32	87.5	3.6	23.8 ± 0.1	34.0 ± 4.9
;;Clk4.1M-GAL4/UAS-DBT(S)	48	91.7	25.0	23.4 ± 0.1	31.6 ± 3.3
;;Clk4.1M-GAL4/UAS-DBT(L)	32	81.3	0	24.0 ± 0.2	18.1 ± 2.6
;Mai179-GAL4/+;	24	87.5	14.3	23.8 ± 0.1	24.5 ± 4.8
;Mai179-GAL4/+;UAS-DBT(S)/+	55	67.3	10.8	22.0 ± 0.5	6.6 ±1.2
;Mai179-GAL4/+;UAS-DBT(L)/+	56	82.1	26.1	25.6 ± 0.1	22.1 ± 2.3
DvPdf-GAL4/Y;;	30	96.7	3.4	24.6 ± 0.2	46.1 ± 4.9
DvPdf-GAL4/Y;;UAS-DBT(S)/+	121	28.1	5.9	20.8 ± 0.9	1.5 ± 0.3
DvPdf-GAL4/Y;;UAS-DBT(L)/+	40	65.0	15.4	27.4 ± 0.1	17.7 ± 3.5
DvPdf-GAL4/Y;Mai179-GAL4/+;	48	54.2	23.1	24.3 ± 0.5	17.6 ± 4.6
DvPdf-GAL4/Y;Mai179-GAL4/+;UAS-DBT(S)/+	127	35.4	2.2	23.2 ± 0.9	2.7 ± 0.5
DvPdf-GAL4/Y;Mai179-GAL4/+;UAS-DBT(L)/+	48	47.9	21.7	26.0 ± 0.5	8.3 ± 2.1
;Mai179-GAL4/+;Clk4.1M-GAL4/+	32	93.8	3.3	23.4 ± 0.2	20.3 ± 3.1
;Mai179-GAL4/+;Clk4.1M-GAL4/UAS-DBT(S)	71	53.5	10.5	21.3 ± 0.6	4.1 ± 0.7
;Mai179-GAL4/+;Clk4.1M-GAL4/UAS-DBT(L)	66	86.4	12.3	26.0 ± 0.1	19.8 ± 2.1

DvPdf-GAL4/Y;;Clk4.1M-GAL4/+	30	100	13.3	23.6 ± 0.1	66.9 ± 7.1
DvPdf-GAL4/Y;;Clk4.1M-GAL4/UAS-DBT(S)	118	37.3	11.4	20.6 ± 0.8	5.3 ± 1.1
DvPdf-GAL4/Y;;Clk4.1M-GAL4/UAS-DBT(L)	70	54.3	15.8	26.6 ± 0.3	8.9 ± 1.6
DvPdf-GAL4/Y;Mai179-GAL4/+;Clk4.1M-GAL4/+	31	83.9	7.7	23.0 ± 0.3	31.8 ± 5.6
DvPdf-GAL4/Y;Mai179-GAL4/+;Clk4.1M-GAL4/UAS-DBT(S)	47	57.4	3.7	17.7 ± 0.6	9.2 ± 1.9
DvPdf-GAL4/Y;Mai179-GAL4/+;Clk4.1M-GAL4/UAS-DBT(L)	48	64.6	12.9	26.0 ± 0.4	12.4 ± 2.9

* % Multi-periodicity indicates the percentage of rhythmic individuals that display more than one significant periodicity.